

Electronic Supplementary Material (ESI) for Journal of Materials Chemistry A. This  
journal is © The Royal Society of Chemistry 2021

## Supporting Information

### **Interfacial engineering of nickel/iron/ruthenium phosphides for efficient overall water splitting powered by solar energy**

*Sheng-Hao Cai, Xiao-Nan Chen, Meng-Jie Huang, Ji-Yuan Han, Yu-Wei Zhou, and Ji-Sen Li\**

*Department of Chemistry and Chemical Engineering, Jining University, Qufu 273155, P. R. China.*

*E-mail: senjili@sina.com*

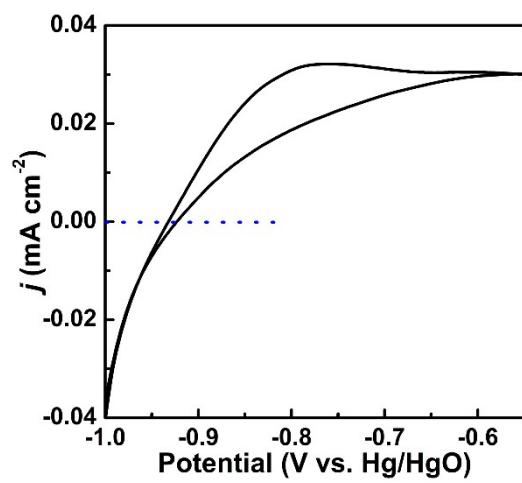


**Fig. S1** Single cycle CV curves of Hg/HgO electrode calibration in 1.0 M KOH.

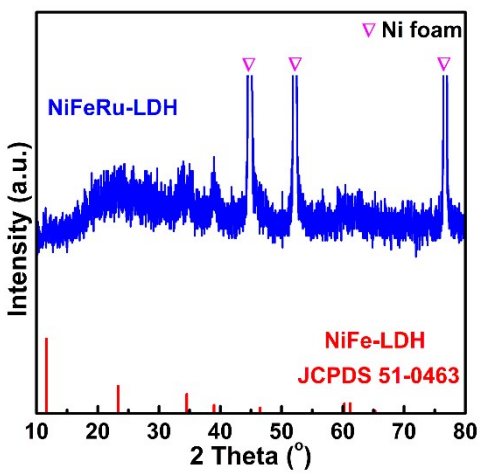


**Fig. S2** PXRD patterns of NiFeRu-LDH.

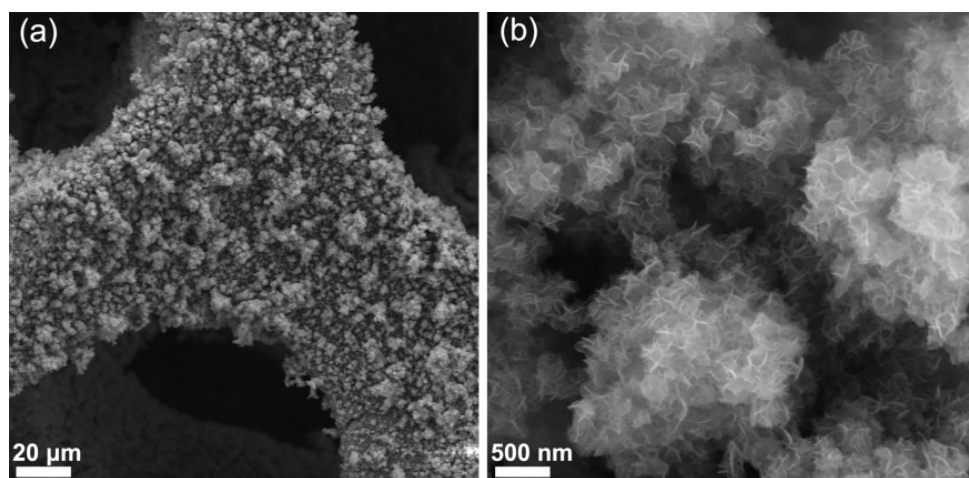


**Fig. S3** (a, b) SEM images of NiFeRu-LDH/NF.

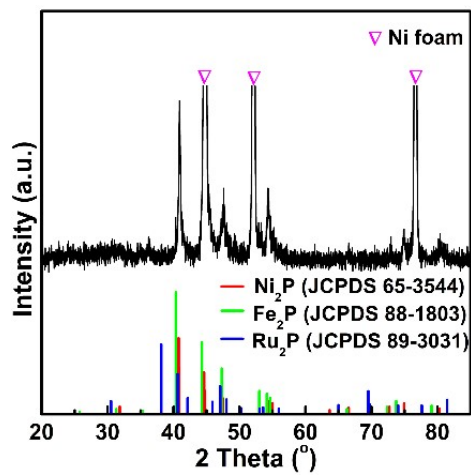


**Fig. S4** PXRD patterns of  $\text{Ni}_2\text{P}$ - $\text{Fe}_2\text{P}$ - $\text{Ru}_2\text{P}$ /NF.

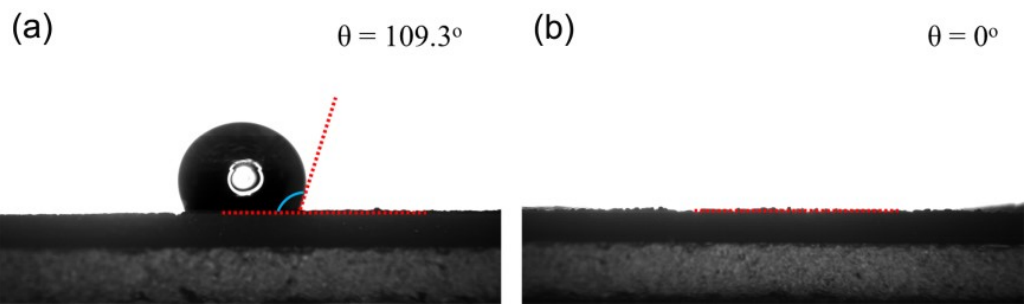


**Fig. S5** Contact angles of NF (a) and  $\text{Ni}_2\text{P}-\text{Fe}_2\text{P}-\text{Ru}_2\text{P}$  /NF (b).

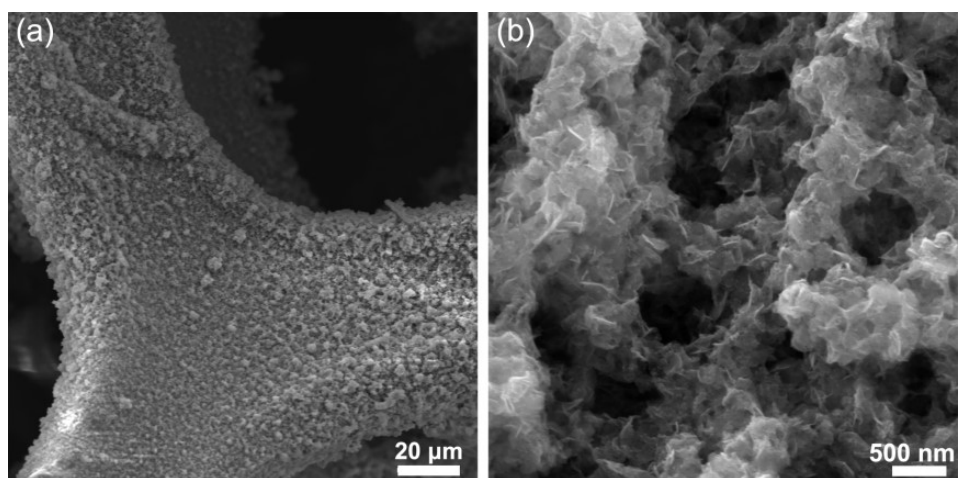


**Fig. S6** (a, b) SEM images of NiFe-LDH/NF.

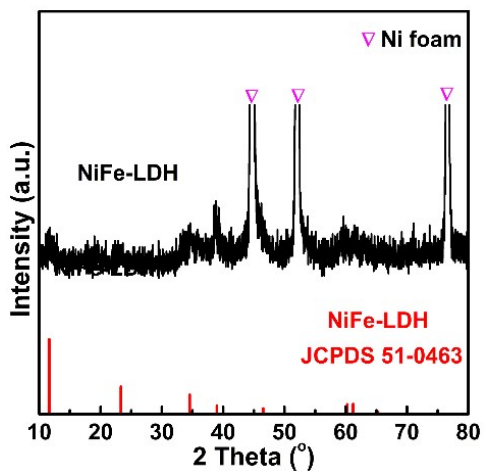


**Fig. S7** PXRD patterns of NiFe-LDH.

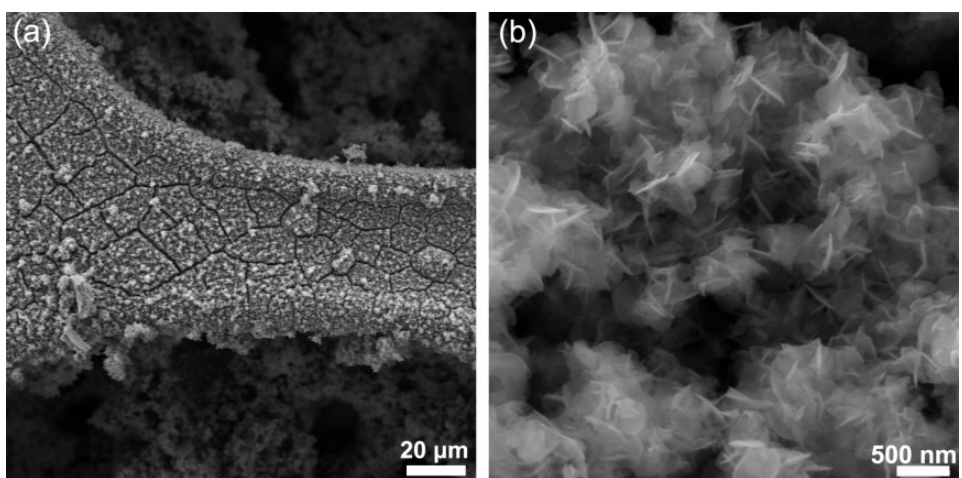


**Fig. S8** (a, b) SEM images of Ni<sub>2</sub>P-Fe<sub>2</sub>P/NF.

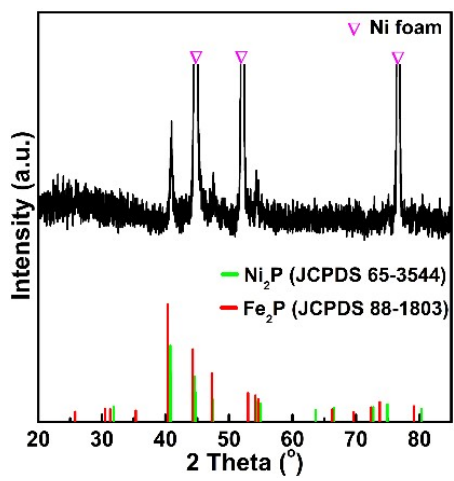


**Fig. S9** PXRD patterns of  $\text{Ni}_2\text{P}-\text{Fe}_2\text{P}/\text{NF}$ .

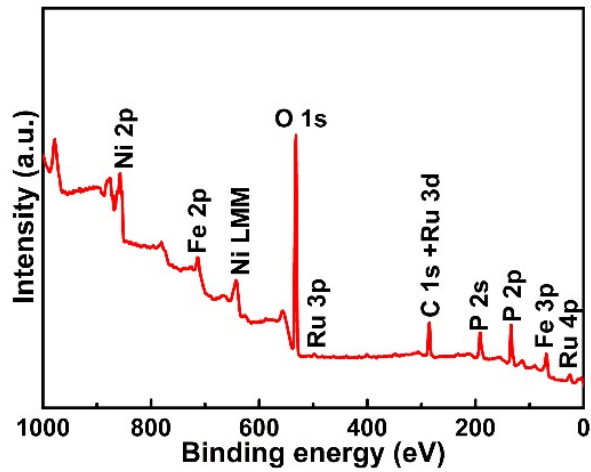


**Fig. S10** The survey XPS spectrum for  $\text{Ni}_2\text{P}-\text{Fe}_2\text{P}-\text{Ru}_2\text{P}/\text{NF}$ .

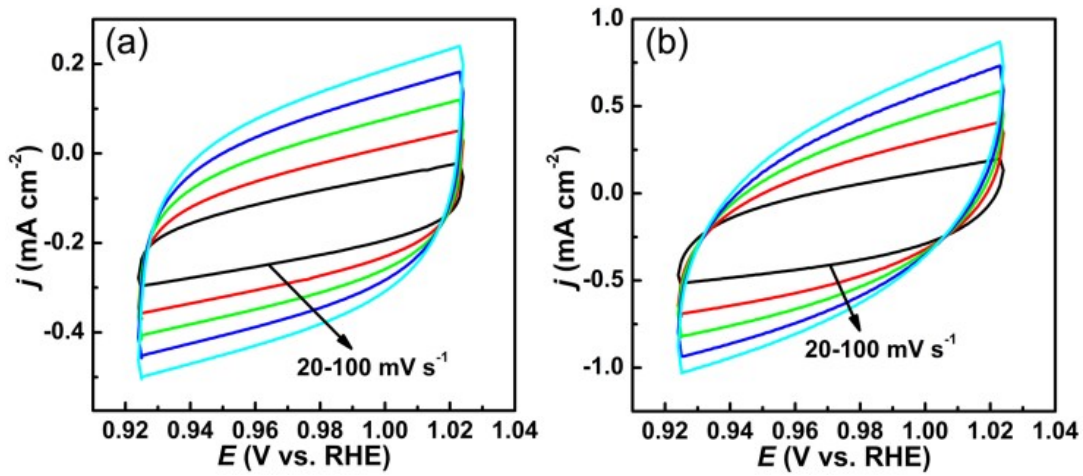


**Fig. S11** CV curves of  $\text{Ni}_2\text{P}-\text{Fe}_2\text{P}/\text{NF}$  (a) and  $\text{Ni}_2\text{P}-\text{Fe}_2\text{P}-\text{Ru}_2\text{P}/\text{NF}$  (b) in the non-Faradaic potential region recorded at different scan rates.

Calculation of ECSA:

$$\text{ECSA} = \frac{C_{dl}}{C_s}$$

$$\text{ECSA}_{\text{Ni}_2\text{P}-\text{Fe}_2\text{P}/\text{NF}} = \frac{2.33 \text{ mF cm}^{-2}}{40 \mu \text{F cm}^{-2}} = 58.3 \text{ cm}^{-2} \text{ ECSA}$$

$$\text{ECSA}_{\text{Ni}_2\text{P}-\text{Fe}_2\text{P}-\text{Ru}_2\text{P}/\text{NF}} = \frac{4.45 \text{ mF cm}^{-2}}{40 \mu \text{F cm}^{-2}} = 111.2 \text{ cm}^{-2} \text{ ECSA}$$

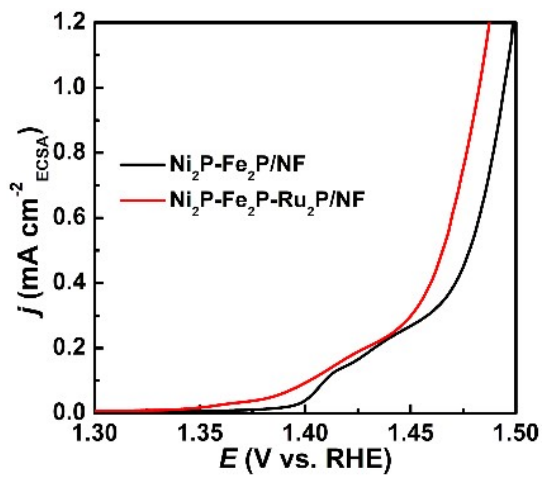


**Fig. S12** OER activity of different catalysts in 1 M KOH normalized by ECSA.

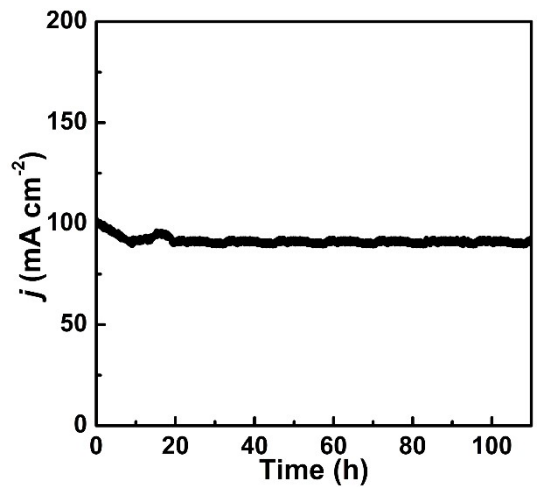


**Fig. S13** Durability test of  $\text{Ni}_2\text{P}-\text{Fe}_2\text{P}-\text{Ru}_2\text{P}/\text{NF}$  at  $100 \text{ mA cm}^{-2}$  for OER.

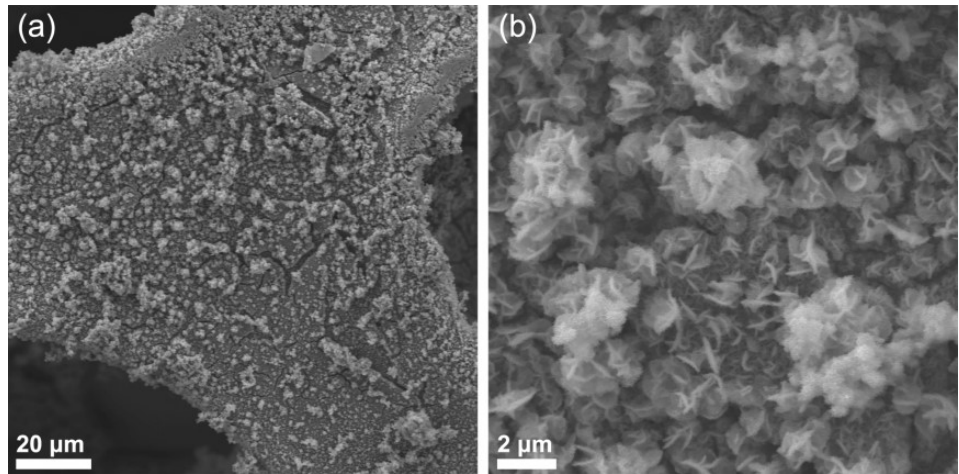


**Fig. S14** (a, b) SEM images of  $\text{Ni}_2\text{P}$ - $\text{Fe}_2\text{P}$ - $\text{Ru}_2\text{P}/\text{NF}$  after OER stability.

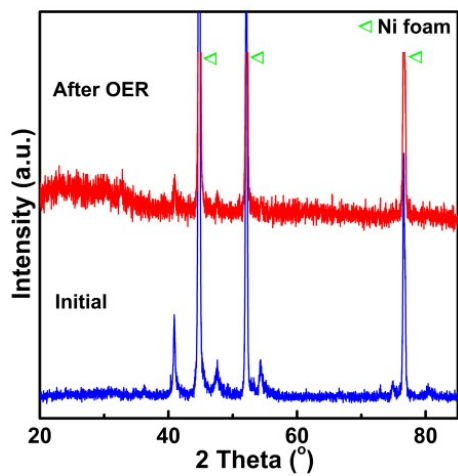


**Fig. S15** PXRD patterns of  $\text{Ni}_2\text{P}-\text{Fe}_2\text{P}-\text{Ru}_2\text{P}/\text{NF}$  before and after stability test for the OER.

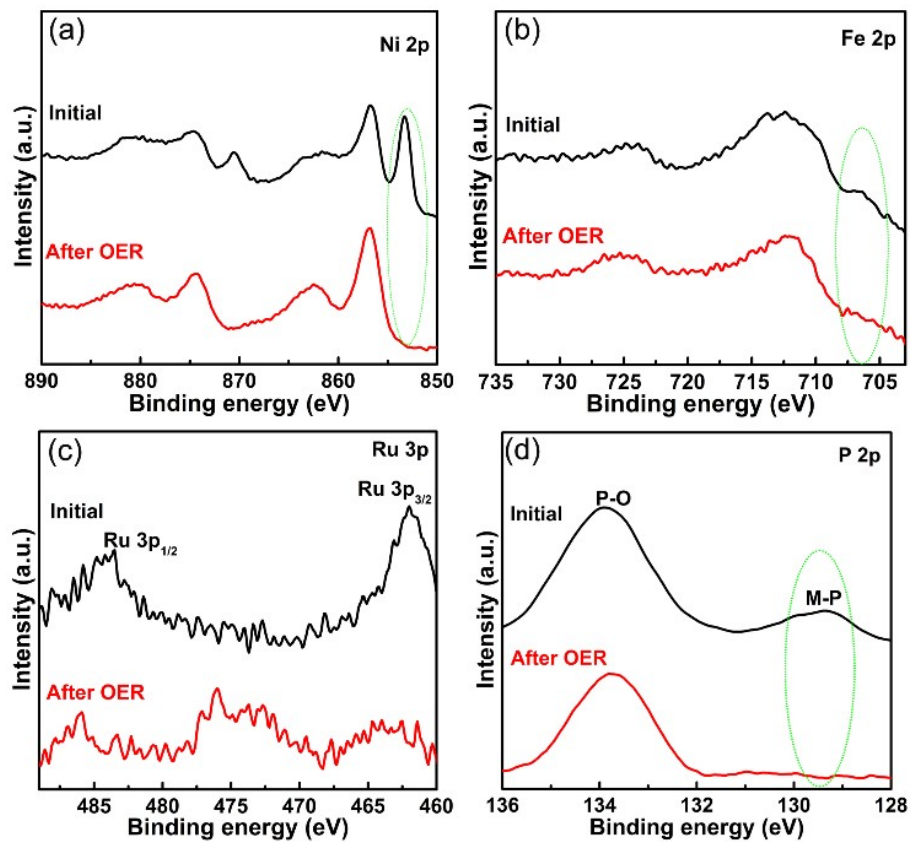


**Fig. S16** High-resolution XPS spectra of (a) Ni 2p, (b) Fe 2p, (c) Ru 3p, and P 2p of  $\text{Ni}_2\text{P}-\text{Fe}_2\text{P}-\text{Ru}_2\text{P}/\text{NF}$  intial and after OER stability testing for the OER.

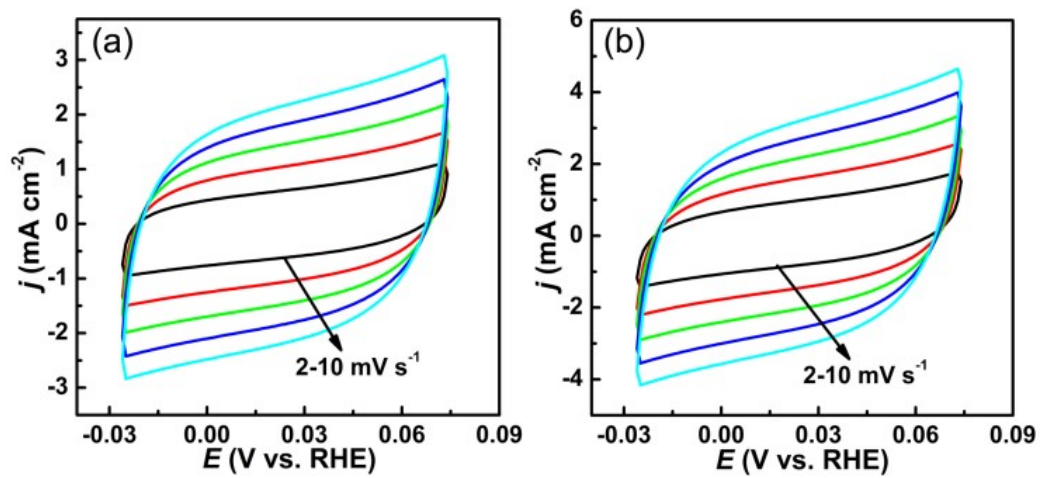


**Fig. S17** CV curves of Ni<sub>2</sub>P-Fe<sub>2</sub>P/NF (a) and Ni<sub>2</sub>P-Fe<sub>2</sub>P-Ru<sub>2</sub>P/NF (b) in the non-Faradaic potential region recorded at different scan rates.

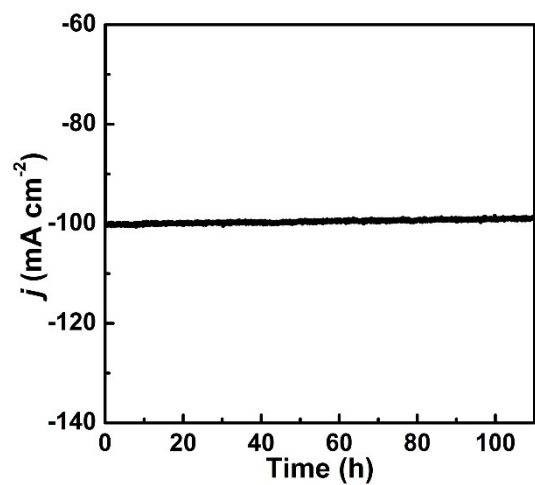


**Fig. S18** Durability test of Ni<sub>2</sub>P-Fe<sub>2</sub>P-Ru<sub>2</sub>P/NF at 100 mA cm<sup>-2</sup> for OER.

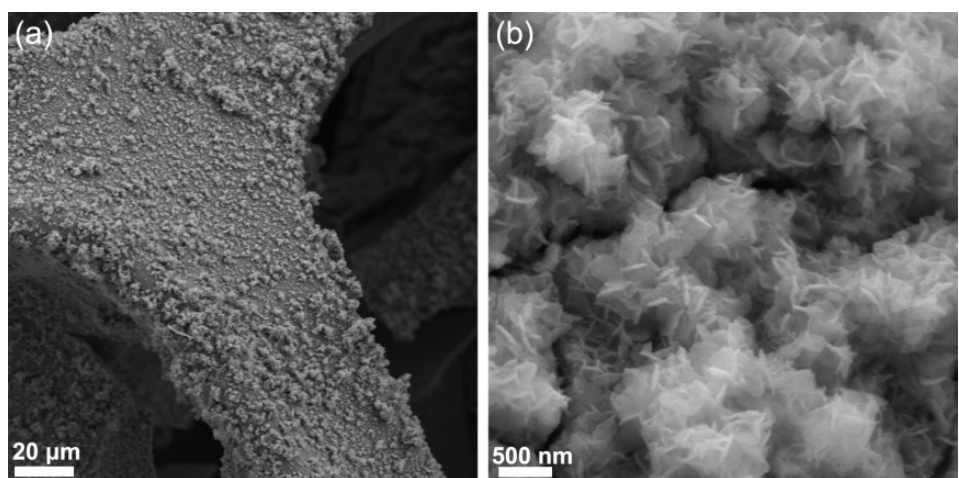


**Fig. S19** (a, b) SEM images of  $\text{Ni}_2\text{P}$ - $\text{Fe}_2\text{P}$ - $\text{Ru}_2\text{P}/\text{NF}$  after the HER stability.

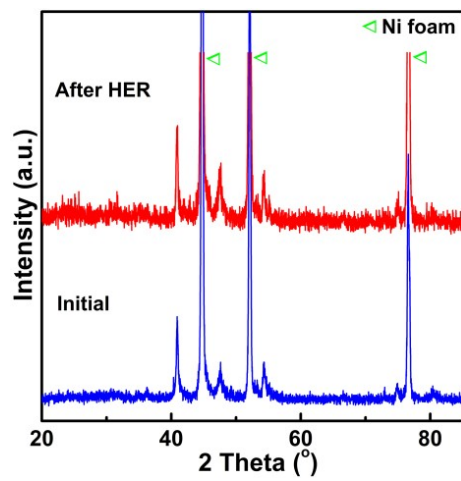


**Fig. S20** PXRD patterns of  $\text{Ni}_2\text{P}-\text{Fe}_2\text{P}-\text{Ru}_2\text{P}/\text{NF}$  before and after stability test for the HER.

**Table S1.** Comparing the electrocatalytic OER performance of Ni<sub>2</sub>P-Fe<sub>2</sub>P-Ru<sub>2</sub>P/NF with many catalysts recently reported.

Catalysts	Tafel slop (mV dec <sup>-1</sup> )	$\eta^{10}$ (mV)	Reference
<b>Ni<sub>2</sub>P-Fe<sub>2</sub>P-Ru<sub>2</sub>P/NF</b>	<b>30.5</b>	<b>195</b>	<b>This work</b>
Mo-Ni <sub>3</sub> S <sub>2</sub> /Ni <sub>x</sub> P <sub>y</sub> /NF	60.6	/	<i>Adv. Energy Mater.</i> 2020, 10, 1903891.
NiMoO <sub>x</sub> /NiMoS	34	186	<i>Nat. Commun.</i> 2020, 11, 5462.
MoS <sub>2</sub> /Co <sub>9</sub> S <sub>8</sub> /Ni <sub>3</sub> S <sub>2</sub> /Ni	58	166	<i>J. Am. Chem. Soc.</i> 2019, 141, 10417
CoMoS <sub>4</sub> /Ni <sub>3</sub> S <sub>2</sub>	63	200	<i>J. Power Sources</i> 2019, 416, 95.
Porous Ni <sub>3</sub> S <sub>4</sub>	67	257	<i>Adv. Funct. Mater.</i> 2019, 29, 1900315.
Co <sub>2</sub> P NCs	60	280	<i>Adv. Mater.</i> 2018, 30, 1705796.
Ni <sub>2</sub> P-CoP	69	320	<i>ACS Appl. Mater. Interfaces</i> 2017, 9, 23222.
NiCoP/C	96	330	<i>Angew. Chem. Int. Ed.</i> 2017, 56, 3897.
MAF-X27-OH	88	292	<i>J. Am. Chem. Soc.</i> 2016, 138, 8336

**Table S2.** Comparing the electrocatalytic HER performance of Ni<sub>2</sub>P-Fe<sub>2</sub>P-Ru<sub>2</sub>P/NF with many catalysts recently reported.

Catalysts	Tafel slop (mV dec <sup>-1</sup> )	$\eta^{10}$ (mV)	Reference
<b>Ni<sub>2</sub>P-Fe<sub>2</sub>P-Ru<sub>2</sub>P/NF</b>	<b>85.1</b>	<b>78.6</b>	<b>This work</b>
Mo-Ni <sub>3</sub> S <sub>2</sub> /Ni <sub>x</sub> P <sub>y</sub> /NF	68.4	109	<i>Adv. Energy. Mater.</i> 2020, 10, 1903891.
CoMoS <sub>4</sub> /Ni <sub>3</sub> S <sub>2</sub>	169	158	<i>J. Power Sources</i> 2019, 416, 95.
Ni <sub>2</sub> P-Fe <sub>2</sub> P/NF	86	128	<i>Adv. Funct. Mater.</i> 2020, 30, 2006484.
NiFeP/NCH	125	216	<i>J. Am. Chem. Soc.</i> 2019, 141, 7906.
MoS <sub>2</sub> /Co <sub>9</sub> S <sub>8</sub> /Ni <sub>3</sub> S <sub>2</sub> /Ni	85	113	<i>J. Am. Chem. Soc.</i> 2019, 141, 10417
(Co <sub>1-x</sub> Ni <sub>x</sub> ) (S <sub>1-y</sub> Py) <sub>2</sub> /G	85	117	<i>Adv. Energy Mater.</i> 2018, 8, 1802319.
Ni <sub>12</sub> P <sub>5</sub> /Ni <sub>3</sub> (PO <sub>4</sub> ) <sub>2</sub> -HS	93.1	114	<i>Appl. Catal. B Environ</i> 2017, 204, 486.

**Table S3.** Comparing the electrocatalytic performance of Ni<sub>2</sub>P-Fe<sub>2</sub>P-Ru<sub>2</sub>P/NF with recently reported catalysts for overall water splitting.

Catalysts	Cell voltage (V)	Reference
<b>Ni<sub>2</sub>P-Fe<sub>2</sub>P-Ru<sub>2</sub>P/NF</b>	<b>1.49</b>	<b>This work</b>
Fe-CoP/Ni(OH) <sub>2</sub>	1.52	<i>Adv. Funct. Mater.</i> 2021, 31, 2101578.
Mo-Ni <sub>3</sub> S <sub>2</sub> /NixPy/NF	1.46	<i>Adv. Energy. Mater.</i> 2020, 10, 1903891.
NiCoP@NiMn LDH/NF	1.51	<i>Appl. Mater. Interfaces</i> 2020, 12, 4385.
Cr-doped FeNiP/NCN	1.5	<i>Adv. Mater.</i> 2019, 31, 1900178.
NiFeP/SG	1.54	<i>Nano Energy</i> 2019, 58, 870.
NiFeP/NCH	1.59	<i>J. Am. Chem. Soc.</i> 2019, 141, 7906.
MoS <sub>2</sub> /Co <sub>9</sub> S <sub>8</sub> /Ni <sub>3</sub> S <sub>2</sub> /Ni	1.54	<i>J. Am. Chem. Soc.</i> 2019, 141, 10417
Mo-doped CoP/CC	1.56	<i>Nano Energy</i> 2018, 48, 73.